



Article

# Iron Overload, Oxidative Stress and Calcium Mishandling in Cardiomyocytes: Role of the Mitochondrial Permeability Transition Pore

Richard Gordan, Nadezhda Fefelova, Judith K. Gwathmey and Lai-Hua Xie \*

Department of Cell Biology and Molecular Medicine, Rutgers University-New Jersey Medical School, Newark, NJ 07103, USA; rgordan48@gmail.com (R.G.); fefelonn@njms.rutgers.edu (N.F.); jgwathmey@gwathmey.com (J.K.G.)

\* Correspondence: xiela@njms.rutgers.edu; Tel.: +1-973-972-2411; Fax: +1-973-972-7489

Received: 20 July 2020; Accepted: 13 August 2020; Published: 16 August 2020



**Abstract:** Iron (Fe) plays an essential role in many physiological processes. Hereditary hemochromatosis or frequent blood transfusions often cause iron overload (IO), which can lead to cardiomyopathy and arrhythmias; however, the underlying mechanism is not well defined. In the present study, we assess the hypothesis that IO promotes arrhythmias via reactive oxygen species (ROS) production, mitochondrial membrane potential ( $\Delta\Psi_m$ ) depolarization, and disruption of cytosolic Ca dynamics. In ventricular myocytes isolated from wild type (WT) mice, both cytosolic and mitochondrial Fe levels were elevated following perfusion with the Fe<sup>3+</sup>/8-hydroxyquinoline (8-HQ) complex. IO promoted mitochondrial superoxide generation (measured using MitoSOX Red) and induced the depolarization of the  $\Delta\Psi_m$  (measured using tetramethylrhodamine methyl ester, TMRM) in a dose-dependent manner. IO significantly increased the rate of Ca wave (CaW) formation measured in isolated ventricular myocytes using Fluo-4. Furthermore, in ex-vivo Langendorff-perfused hearts, IO increased arrhythmia scores as evaluated by ECG recordings under programmed S1-S2 stimulation protocols. We also carried out similar experiments in cyclophilin D knockout (CypD KO) mice in which the mitochondrial permeability transition pore (mPTP) opening is impaired. While comparable cytosolic and mitochondrial Fe load, mitochondrial ROS production, and depolarization of the  $\Delta\Psi_m$  were observed in ventricular myocytes isolated from both WT and CypD KO mice, the rate of CaW formation in isolated cells and the arrhythmia scores in ex-vivo hearts were significantly lower in CypD KO mice compared to those observed in WT mice under conditions of IO. The mPTP inhibitor cyclosporine A (CsA, 1  $\mu$ M) also exhibited a protective effect. In conclusion, our results suggest that IO induces mitochondrial ROS generation and  $\Delta\Psi_m$  depolarization, thus opening the mPTP, thereby promoting CaWs and cardiac arrhythmias. Conversely, the inhibition of mPTP ameliorates the proarrhythmic effects of IO.

**Keywords:** iron overload; oxidative stress; calcium dynamics; heart; mitochondria; arrhythmia

## 1. Introduction

Iron overload (IO) conditions can be found in patients with hereditary hemochromatosis or in patients receiving frequent blood transfusions (e.g., for treating sickle cell disease or thalassemia). For example, patients suffering from hemochromatosis are genetically predisposed to absorb excessive dietary Fe and thus build up high plasma Fe levels. The resultant non-transferrin bound iron accumulates in organs and tissues, leading to organ damage and potentially organ failure. It has been suggested that IO leads to cardiomyopathy and heart failure [1–3], and its role in cardiac arrhythmogenesis remains controversial [4,5]

Recent studies have pointed towards IO as a potential contributor to mitochondrial dysfunction [6–8]. One mechanism by which Fe damages cardiomyocytes is thought to be mediated by excess reactive oxygen species (ROS) within mitochondria and/or the cytosol via the Fenton reaction [5,9]. A strong connection between ROS and cardiac diseases including heart failure, hypertrophy, and arrhythmias has been suggested [10–13]. Furthermore, mitochondria have been shown to play a vital role in cardiomyocyte intracellular Ca homeostasis [14–16].

Mitochondrial Ca efflux is primarily dependent on two mechanisms: the Na-Ca exchanger, which is the primary channel under physiologic conditions, and the mitochondrial permeability transition pore (mPTP) which opens during times of pathophysiologic stress [17]. These Ca channels/transporters get their driving force from the Ca gradient and mitochondrial membrane potential ( $\Delta\Psi_m$ ) established by the proton gradient generated by the mitochondrial electron transport chain.

It has also been shown that mitochondria are physically associated with the sarcoplasmic reticulum (SR) [18]. This link is approximately 10 to 50 nm wide and may thus create micro-domains in which the intracellular Ca levels can be readily manipulated to induce a variety of ionic fluxes. Our previous study suggests that mitochondrial Ca efflux creates a micro-domain with an increase in local Ca between the ryanodine receptors and the SR Ca ATPase uptake channels, thereby altering the Ca handling properties of the SR and in the cytosol [19]. We have shown that the protonophore carbonyl cyanide *p*-(trifluoromethoxy) phenylhydrazone (FCCP) leads to  $\Delta\Psi_m$  depolarization and mPTP opening, which subsequently allows for mitochondrial Ca release via the mPTP. The release of mitochondrial Ca promotes spontaneous Ca release from the SR, resulting in Ca waves (CaWs), which eventually promotes the generation of triggered electrical activities and arrhythmogenesis [19]. More recently, by using cyclosporin A (CsA), a selective inhibitor of mPTP, or the cyclophilin D knockout (CypD KO) mouse model, we have further demonstrated that inhibition of mPTP can attenuate FCCP-induced mitochondrial Ca efflux and subsequently prevent the occurrence of CaWs in ventricular myocytes as well as reduce the incidence of arrhythmias at the whole heart level [20]. However, a link between IO, mitochondrial mPTP activity, and cytosolic Ca mobilization has not been demonstrated to date. In the present study, we demonstrate that IO promotes ROS production, resulting in  $\Delta\Psi_m$  depolarization. As a result, there is mitochondrial Ca efflux via mPTP which ultimately promotes CaW formation and arrhythmogenesis. For our studies, we have used both pharmacological (CsA) and genetic (CypD KO) approaches to inhibiting mPTP function.

## 2. Materials and Methods

### 2.1. Animal Models

As we described in our previous study [20], WT and CypD KO [21] mice (2–4 months, either gender) were purchased from The Jackson Laboratories (Bar Harbor, ME, USA). All animal experimental protocols were reviewed by the Institutional Animal Care and Use Committee at Rutgers New Jersey Medical School and were in accordance with the Guide for the Care and Use of Laboratory Animals published by the National Institutes of Health (Revised 1996, The Animal Welfare Assurance Number D16-00098; IACUC Protocol #: PROTO999901063).

### 2.2. Chemicals and Reagents

Most chemicals and reagents were purchased from Sigma-Aldrich (St. Louis, MO, USA) or Invitrogen by Thermo Fisher Scientific (Grand Island, NY, USA), as indicated. Hydrophobic reagents were dissolved in DMSO and then diluted to working concentrations in normal Tyrode's solution. The maximum DMSO concentration was <0.2% by volume. A membrane permeable complex of  $\text{Fe}^{3+}$  and 8-hydroxyquinoline (8-HQ, Sigma-Aldrich) was used to iron load ventricular myocytes. It has been reported that, after the lipophilic  $\text{Fe}^{3+}$ /8-HQ complex enters into the cell,  $\text{Fe}^{3+}$  ions undergo rapid intracellular reduction to  $\text{Fe}^{2+}$  [22]. Cytosolic  $\text{Fe}^{3+}$  and  $\text{Fe}^{2+}$  then become part of the pool of labile Fe within the cell, i.e., chelatable and redox-active [23].

### 2.3. Cell Isolation

Left ventricular myocytes were enzymatically isolated from mouse hearts, as described previously [24–26]. Briefly, the hearts were removed from mice deeply anesthetized with isoflurane (Henry Schein Animal Health, Dublin, OH, USA) and were retrogradely perfused at 37 °C in Langendorff fashion with nominally Ca-free Tyrode's solution containing 0.5 mg/mL collagenase (Type II; Worthington Biochemical Co., Lakewood, NJ, USA) and 0.1 mg/mL thermolysin (Sigma-Aldrich) for 10–12 min. The enzyme solution was then washed out and the hearts were removed from the perfusion apparatus. The left ventricle was removed and placed in a petri dish. Myocytes were isolated after being teased apart using forceps and being filtered through a nylon mesh. The Ca concentration was gradually increased to 1.0 mM and the cells were stored at room temperature. Ventricular myocytes were studied within 8 h of isolation.

### 2.4. Measurement of Cytosolic and Mitochondrial Fe Loading

To determine cytosolic ferrous iron ( $\text{Fe}^{2+}$ ) loading, ventricular myocytes were loaded with 40  $\mu\text{M}$  Phen Green SK (Invitrogen) for 10 min at room temperature. In order to determine mitochondrial  $\text{Fe}^{2+}$ , ventricular myocytes were loaded with 5  $\mu\text{M}$  rhodamine B-[(1,10-phenanthroline-5-yl)-aminocarbonyl]benzyl ester (RPA; Squarix Biotechnology by Axxora, Recklinghausen, Germany) for 20 min at 37 °C. Fluorescence (Ex/Em: 484/520 nm for Phen Green and 543/560 nm for RPA) was monitored using an Eclipse TE200 inverted microscope (Nikon, Tokyo, Japan) and recorded using an Ixon Charge-Coupled Device (CCD) camera (Andor Technology, Concord, MA, USA).

### 2.5. Measurement of Mitochondrial Reactive Oxygen Species Levels

Ventricular myocytes were loaded with 5  $\mu\text{M}$  MitoSOX Red (Invitrogen) for 30 min at 37 °C in order to visualize mitochondrial superoxide production. The fluorescence (Ex/Em: 485/585 nm) was monitored and presented as background-subtracted  $F/F_0$  values. The  $F/F_0$  value was expressed as "0" during the periods when the cell was not exposed to the excitation light. The baseline value (before perfusion of  $\text{Fe}^{3+}$ /8-HQ) was normalized to 1. The results were obtained every 2 min by averaging 3 consecutive 200-ms exposures.

### 2.6. Measurement of Mitochondrial Membrane Potential

Isolated ventricular myocytes were loaded with 50 nM tetramethylrhodamine methyl ester (TMRM, Invitrogen) at 37 °C for 40 min. Fluorescence (Ex/Em: 548/570 nm) was monitored and stored. A decrease in fluorescence rate was used as an index of mitochondrial membrane depolarization [19].

### 2.7. Measurements of Intracellular Ca Fluorescence

Ventricular myocytes were loaded with Fluo-4-AM (4  $\mu\text{M}$ ) (Invitrogen) for 40 min at room temperature, after which the incubating solution was removed and fresh Tyrode's solution was added. Fluorescence (Ex/Em: 485/530 nm) was monitored as described in our previous studies [11,27]. Ca fluorescence intensity was recorded as the ratio  $F/F_0$  (fluorescence ( $F$ ) over the basal diastolic fluorescence ( $F_0$ )).

### 2.8. Electrocardiograms (ECG) and Arrhythmia Induction Testing

Electrocardiograms (ECGs) were recorded at a sampling rate of 1 kHz in Langendorff-perfused hearts by placing an Ag-AgCl electrode pair close to the apex and on the right atrial appendage to produce a pseudo-lead II. Additionally, two platinum electrodes were placed on the right ventricular free wall for electrical stimulation (Grass Instruments, West Warwick, RI, USA). The hearts were perfused with normal Tyrode's solution at 37 °C. The S1-S2 programmed electrical stimulation protocol (S1 being the regular train pulse and S2 the premature stimulus) at twice the pacing threshold intensity was used [20,26]. After a 20-beat train with 100-ms cycle length (S1), 3 repeated sets of 3

extra stimuli (S2) with cycle lengths of 50, 40, and 30 ms were introduced. Arrhythmia scores were assigned as follows: 0, no arrhythmia; 1 point, 1–3 premature ventricular contractions (PVCs); 2 points, non-sustained ventricular tachycardia (VT) (4–10 consecutive PVCs, including bigeminal or trigeminal PVCs); 3 points, sustained VT (>10 consecutive PVCs); 4 points, ventricular fibrillation (VF) or sudden cardiac arrest (SCD).

### 2.9. Statistics

Individual groups were compared by Student's *t*-tests or Fischer's exact tests, as indicated in the text. Results were considered statistically significant if the *p* value was less than 0.05. Results were expressed as mean  $\pm$  SEM.

## 3. Results

### 3.1. Fe Load in the Cytosol and Mitochondria in WT and CypD KO Ventricular Myocytes

In order to establish IO, we mixed  $\text{Fe}^{3+}$  with the cell permeable molecule 8-hydroxyquinoline to form a  $\text{Fe}^{3+}/8\text{-HQ}$  complex. To confirm that  $\text{Fe}^{3+}/8\text{-HQ}$  is capable of readily entering the cell and that  $\text{Fe}^{3+}$  is reduced to  $\text{Fe}^{2+}$ , we used Phen Green SK to visualize cytosolic  $\text{Fe}^{2+}$  levels and RPA to visualize mitochondrial  $\text{Fe}^{2+}$  levels. The baseline fluorescence levels (arbitrary units, AU) were normalized to 100%. As shown in Figure 1A,C, in WT myocytes, the treatment with  $\text{Fe}^{3+}/8\text{-HQ}$  resulted in a rapid decrease (quenching) in Phen Green SK fluorescence ( $54.4 \pm 4.5\%$ ), indicating that cytosolic  $\text{Fe}^{2+}$  was increased. Upon addition of the cell-permeable Fe chelator 2,2'-bipyridyl (BPD, 5 mM), fluorescence was restored to  $118.4 \pm 16.9\%$  after 15 min (Figure 1A,C), indicating that labile Fe in the cytosol was successfully chelated by BPD, which is a strong cytosolic Fe chelator. The same experiments were conducted in ventricular myocytes isolated from CypD KO mice. As shown in Figure 1B,C, the treatment with  $\text{Fe}^{3+}/8\text{-HQ}$  resulted in a significant decrease in Phen Green SK fluorescence to  $36.9 \pm 7.2\%$ , which was recovered to  $126.7 \pm 23.3\%$  after chelation with BPD. To determine whether mitochondrial  $\text{Fe}^{2+}$  level was elevated as well after  $\text{Fe}^{3+}/8\text{-HQ}$  treatment, we monitored the fluorescence of RPA that is considered to be specific to mitochondrial  $\text{Fe}^{2+}$ . As seen in Figure 1D,F, the average fluorescence of RPA in WT myocytes was significantly decreased to  $34.8 \pm 2.7\%$  when the cells were perfused with  $15 \mu\text{M}$   $\text{Fe}^{3+}/8\text{-HQ}$ , suggesting that mitochondrial  $\text{Fe}^{2+}$  was increased. BPD has also been reported to be a mitochondria-accessible Fe chelator [28]. When treated with BPD, a partial recovery of RPA fluorescence was observed ( $58.4 \pm 5.4\%$ ), suggesting partial chelation of mitochondrial  $\text{Fe}^{2+}$ . The same experiments were conducted in myocytes isolated from CypD KO mice. As shown in Figure 1E,F, the average fluorescence of RPA in CypD KO myocytes was not different from WT at baseline. After treatment with  $15 \mu\text{M}$   $\text{Fe}^{3+}/8\text{-HQ}$ , RPA fluorescence was significantly decreased to  $30.7 \pm 3.0\%$  in CypD KO, which was recovered to  $66.2 \pm 11.2\%$  with the addition of BPD. These results clearly show that  $\text{Fe}^{3+}/8\text{-HQ}$  treatment generates an IO condition in both WT and CypD ventricular myocytes, resulting in an increase in both cytosolic and mitochondrial  $\text{Fe}^{2+}$  levels.

### 3.2. IO induced Mitochondrial ROS Generation and $\Delta\Psi_m$ Depolarization

We next sought to evaluate mitochondrial ROS production in ventricular myocytes in the presence of IO. Perfusion with  $\text{Fe}^{3+}/8\text{-HQ}$  ( $15 \mu\text{M}$ ) significantly increased the fluorescence of MitoSOX Red, a mitochondrial ROS sensitive dye (Figure 2A–C). In both WT (Figure 2A) and CypD KO mouse myocytes (Figure 2B), fluorescence was increased, indicating that IO significantly increases mitochondrial ROS production. No significant difference was found between WT and CypD KO ventricular myocytes.  $\text{H}_2\text{O}_2$  was used as a positive control following addition of  $15 \mu\text{M}$   $\text{Fe}^{3+}/8\text{-HQ}$ . Addition of  $1 \text{ mM}$   $\text{H}_2\text{O}_2$  resulted in a further increase in mitochondrial ROS levels, potentially indicating that the relative maximum level of mitochondrial ROS generation was attained.

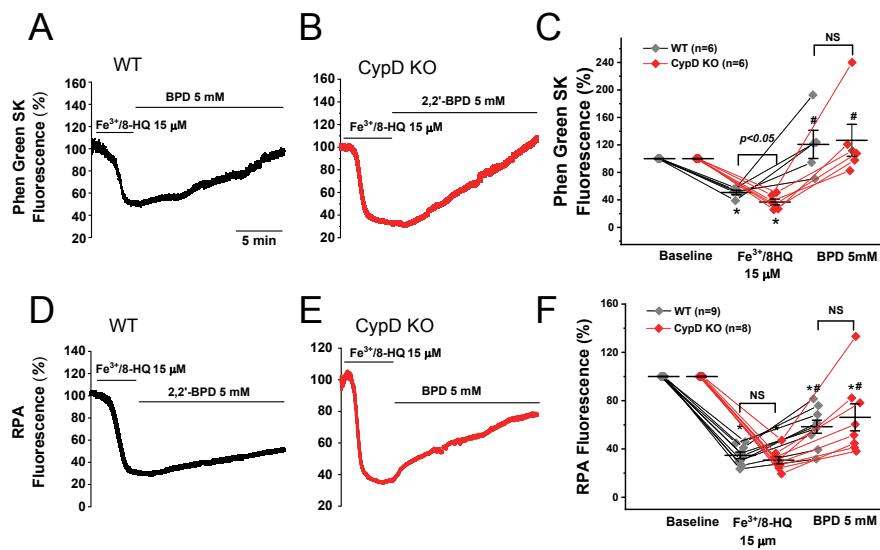


**Figure 1.** Cytosolic and mitochondrial Fe loading in ventricular myocytes isolated from WT and CypD KO mice. The level of cytosolic Fe was measured using Phen Green SK fluorescence in WT (A) and CypD KO myocytes (B). The baseline fluorescence levels (arbitrary units, AU) were normalized to 100%. Cytosolic Fe loading was achieved by continuous superfusion with 15  $\mu$ M  $Fe^{3+}/8-HQ$ . Decreased fluorescence intensity of Phen Green SK indicated the increase in cytosolic Fe levels. Note that the quenched fluorescence was reversed in the presence of the membrane-permeable Fe chelator 2,2'-bipyridyl (BPD). Summarized data (C) were obtained from 6 WT cells and 6 CypD KO cells, respectively. Similarly, mitochondrial Fe loading was measured by using rhodamine B-[1,10-phenanthroline-5-yl]-aminocarbonyl]benzyl ester (RPA) fluorescence in WT (D) and CypD KO myocytes (E). Data are summarized in (F). Data were obtained from 9 WT cells and 8 CypD KO ventricular myocytes. \*  $p < 0.05$  compared to the baseline in WT and CypD, respectively; #  $p < 0.05$  compared to the  $Fe^{3+}/8-HQ$  treatment group in WT and CypD, respectively, by using paired *t*-test. Except for  $Fe^{3+}/8-HQ$ -induced Phen Green SK fluorescence, no significant difference was observed between WT and CypD KO.

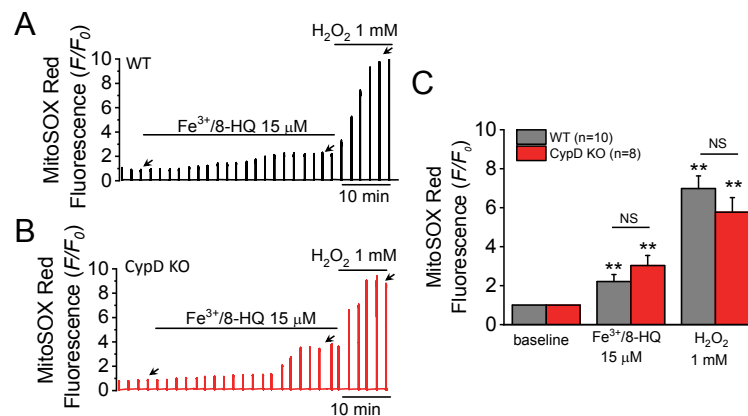


**Figure 2.** Fe-induced reactive oxygen species (ROS) generation in ventricular myocytes isolated from WT and CypD KO mice. Increases in MitoSOX Red fluorescence were used as an indicator of mitochondrial superoxide production. MitoSOX Red fluorescence traces were recorded in a WT (A) and a CypD KO myocyte (B) treated with 15  $\mu$ M  $Fe^{3+}/8-HQ$ . The baseline value was normalized to 1, as indicated by the left-most arrow in each panel. The effect of Fe treatment was measured at the point indicated by the middle arrow.  $H_2O_2$  (1 mM) was used as a positive control indicator. Summary data (C) were obtained from 10 WT and 8 CypD KO myocytes, \*\*  $p < 0.01$  compared to baseline in WT and CypD KO group, respectively, by using paired *t*-test. NS: no significant difference was observed between WT and CypD KO groups by unpaired *t*-test.

Next, we assessed  $\Delta\Psi_m$ . As shown in Figure 3,  $\Delta\Psi_m$  was monitored by TMRM fluorescence in WT (Figure 3A–C) and CypD KO (Figure 3D,E) myocytes. Myocyte membrane potential was depolarized with the addition of  $\text{Fe}^{3+}/8\text{-HQ}$  in a dose- and time-dependent manner in both WT and CypD KO myocytes. While  $\text{Fe}^{3+}/8\text{-HQ}$  at a low concentration (1  $\mu\text{M}$ ) caused less depolarization, 15  $\mu\text{M}$   $\text{Fe}^{3+}/8\text{-HQ}$  induced significant depolarization starting at 2 min and reached quasi-maximal effect at 8 min after treatment. We fitted data at the eight-minute time point to the Hill equation (see figure legend for details). As shown in Figure 3C, the half maximal effective concentration ( $\text{EC}_{50}$ ) was  $6.3 \pm 0.3 \mu\text{M}$  of  $\text{Fe}^{3+}/8\text{-HQ}$  for depolarization of the  $\Delta\Psi_m$ , while the Hill coefficient ( $n_H$ ) was  $2.7 \pm 0.2$  in WT myocytes. In CypD KO myocytes (Figure 3D,E), we obtained an  $\text{EC}_{50}$  of  $7.2 \pm 0.4 \mu\text{M}$  and  $n_H$  of  $2.7 \pm 0.1$ , which were not significantly different from WT. These results suggest that IO may cause the same level of depolarization of mitochondrial  $\Delta\Psi_m$  in both WT and CypD KO myocytes.

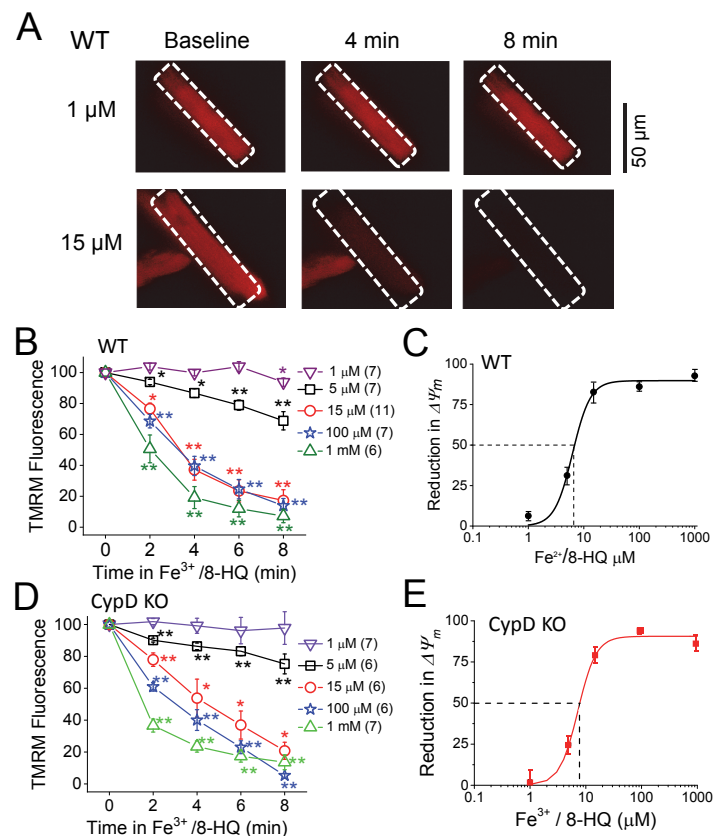


**Figure 3.** Fe-induced depolarization of mitochondrial membrane potential ( $\Delta\Psi_m$ ) in ventricular myocytes isolated from WT and CypD KO mice. (A) Representative snapshots of WT myocytes loaded with TMRM at baseline and 4 and 8 min after being treated with 1 and 15  $\mu\text{M}$   $\text{Fe}^{3+}/8\text{-HQ}$ . (B) Summarized data showing a decrease in tetramethylrhodamine methyl ester (TMRM) fluorescence over time after Fe treatment in WT. The numbers of myocytes used in the measurement are indicated. (C) Percentile depolarization of  $\Delta\Psi_m$  at 8 min after Fe treatment in WT fit to Hill equation:  $\Delta\Psi_m = \Delta\Psi_{m, \max} * [\text{Fe}]^{n_H} / (\text{EC}_{50}^{n_H} + [\text{Fe}]^{n_H})$ . Half maximal effective dose ( $\text{EC}_{50}$ ) and Hill coefficient ( $n_H$ ) are  $6.3 \pm 0.3 \mu\text{M}$  and  $2.7 \pm 0.2$ , respectively, for WT. (D,E) In CypD KO myocytes, same as (B and C).  $\text{EC}_{50}$  and  $n_H$  are  $7.2 \pm 0.4$  and  $2.7 \pm 0.1$  for CypD KO. \*  $p < 0.05$ , \*\*  $p < 0.01$  compared to the respective baseline value. Carbonyl cyanide *p*-(trifluoromethoxy) phenylhydrazone (FCCP, 30  $\mu\text{M}$ ) was used to completely dissipate the  $\Delta\Psi_m$  after the Fe treatment in each recording (not shown).

### 3.3. Promotion of Ca Waves by IO and Protection by mPTP Inhibition

In a previous study, we demonstrated that depolarization of  $\Delta\Psi_m$  (by FCCP) promotes CaW generation, presumably by opening mPTP that releases mitochondrial Ca and triggers SR Ca

release [19,20]. We next tested whether IO might also accelerate CaW formation via mPTP activation. As shown in Figure 4A,B,  $\text{Fe}^{3+}/8\text{-HQ}$  significantly increased the frequency of CaW formation in a dose-dependent manner in WT ventricular myocytes. The frequency of formation of CaWs increased from  $21.4 \pm 1.9$  to  $44.7 \pm 5.3 \text{ min}^{-1}$  ( $p < 0.01$ ) at  $15 \mu\text{M}$ , while it was further increased to  $56.2 \pm 4.1 \text{ min}^{-1}$  ( $p < 0.01$ ) at  $100 \mu\text{M}$ . To determine the role of mPTP, we studied ventricular myocytes from CypD KO mouse hearts which have impaired mPTP function [21]. As shown in Figure 4C,D, CypD KO myocytes perfused with the same concentrations of  $\text{Fe}^{3+}/8\text{-HQ}$  showed no significant increase in the frequency of formation of CaWs (from baseline  $26.0 \pm 3.2 \text{ min}^{-1}$  to  $27.3 \pm 3.8 \text{ min}^{-1}$  at  $15 \mu\text{M}$  and  $28.4 \pm 4.6 \text{ min}^{-1}$  at  $100 \mu\text{M}$ ,  $p > 0.05$ ). The dose-dependent increase in the frequency of CaW formation in WT myocytes was abrogated by pretreatment with CsA, a selective mPTP blocker. As shown in Figure 4E,F,  $\text{Fe}^{3+}/8\text{-HQ}$  did not cause a significant increase in the frequency of CaW formation in the presence of  $1 \mu\text{M}$  CsA ( $28.6 \pm 6.7 \text{ min}^{-1}$  to  $30.0 \pm 7.2 \text{ min}^{-1}$  at  $5 \mu\text{M}$ , and  $29.1 \pm 6.9 \text{ min}^{-1}$  at  $15 \mu\text{M}$ ,  $p > 0.05$ ). However,  $1 \mu\text{M}$  CsA did not completely abolish the effect of  $\text{Fe}^{3+}/8\text{-HQ}$  at the higher concentration of  $\text{Fe}^{3+}/8\text{-HQ}$  ( $100 \mu\text{M}$ ).  $\text{Fe}^{3+}/8\text{-HQ}$  at  $100 \mu\text{M}$  resulted in a slight but significant increase in the frequency of CaW formation ( $28.6 \pm 6.7 \text{ min}^{-1}$  vs  $37.6 \pm 9.2 \text{ min}^{-1}$ ,  $p < 0.05$ ). Taken together, these results suggest that mPTP-mediated Ca release from mitochondria may contribute to IO-induced CaW formation. Inhibition of mPTP function by either pharmacologic (CsA) or genetic (CypD KO) approaches attenuated CaW formation.

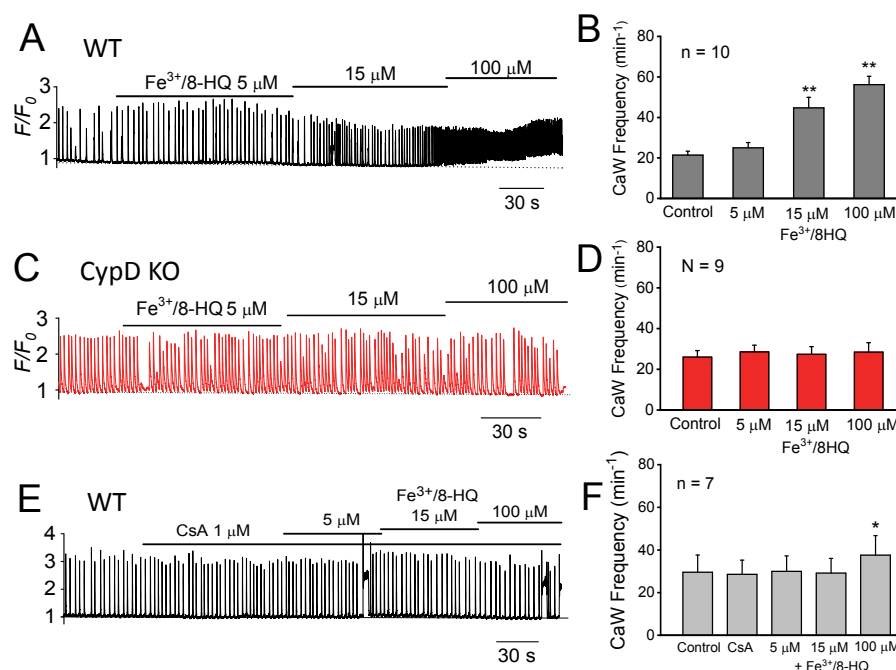


**Figure 4.** Promotion of Ca wave generation by Fe and attenuation by mitochondrial permeability transition pore (mPTP) Inhibition. (A) A representative Ca fluorescence trace showing the effect of  $\text{Fe}^{3+}/\text{HQ-8}$  (5, 15, and  $100 \mu\text{M}$ ) on the frequency of spontaneous Ca wave formation in a WT ventricular myocyte. (B) Summarized data obtained from 10 WT myocytes. (C,D) The same as (A,B), except in CypD KO ventricular myocytes ( $n = 9$ ). (E,F) The same as (A,B), except that the WT myocytes were pretreated with  $1 \mu\text{M}$  CsA before Fe perfusion ( $n = 7$ ). \*  $p < 0.05$ , \*\*  $p < 0.01$ , compared to respective control value by paired  $t$ -test.

### 3.4. Preventative Effect of Antioxidants against IO Toxicity

To further examine the contribution of an increase in the production of ROS to CaW formation resulting from IO, we tested the possible preventative effect of EUK-8, a strong synthetic antioxidant that exhibits both superoxide dismutase and catalase activities. As shown in Figure 5A,B, we pretreated ventricular myocytes with  $50 \mu\text{M}$  EUK-8 for 2 min, followed by concurrent perfusion with  $\text{Fe}^{3+}/8\text{-HQ}$  for

eight minutes. Although  $\text{Fe}^{3+}/8\text{-HQ}$  treatment still depolarized  $\Delta\Psi_m$  (decrease in TMRM fluorescence) in the presence of 50  $\mu\text{M}$  EUK-8, the extent of depolarization was weaker than what we observed in the control group. Furthermore, treatment with  $\text{Fe}^{3+}/8\text{-HQ}$  (15  $\mu\text{M}$ ) resulted in no significant increase in mitochondrial superoxide generation (as monitored by MitoSOX Red) in the presence of EUK-8 (Figure 5C,D). The effect of subsequent treatment with exogenous  $\text{H}_2\text{O}_2$  (1 mM) was also attenuated by EUK-8. More importantly, as shown in Figure 5E,F, pretreatment with EUK-8 prevented an increase in the frequency of CaW formation seen with 15  $\mu\text{M}$   $\text{Fe}^{3+}/8\text{-HQ}$ . Similar results with regard to ROS and CaW formation were also observed in cells pretreated with 20  $\mu\text{M}$  MitoTEMPO (a mitochondrial-targeted superoxide scavenger) (data not shown). These results clearly reveal that antioxidants can attenuate IO-induced mitochondrial ROS production,  $\Delta\Psi_m$  depolarization, and CaW formation.

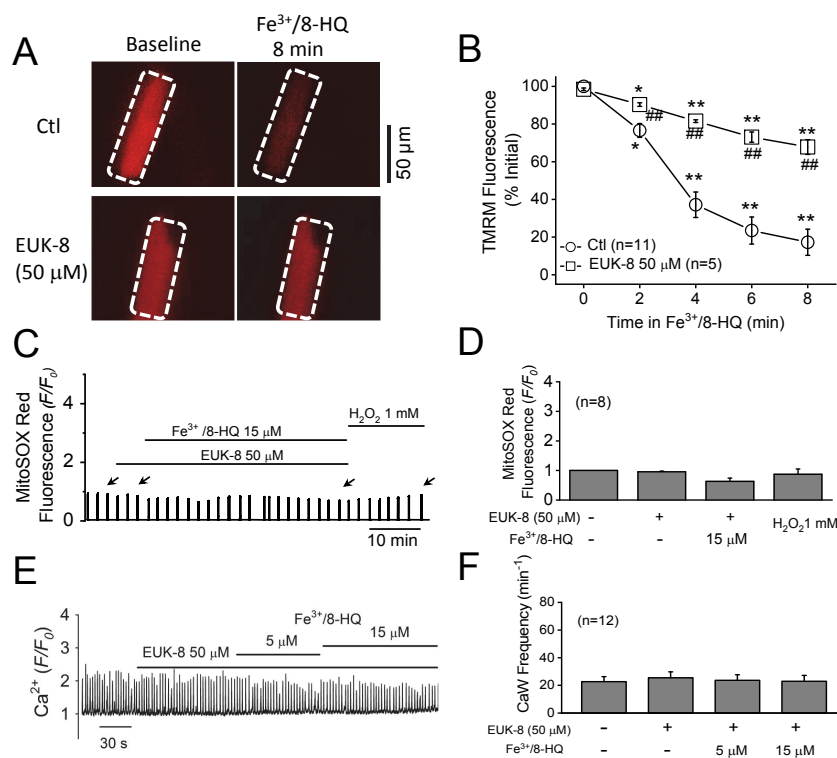


**Figure 5.** Attenuation of Fe-induced mitochondrial dysfunction and Ca waves by antioxidants. (A) Representative snapshots of WT myocytes loaded with TMRM at baseline and 8 min after being treated with 15  $\mu\text{M}$   $\text{Fe}^{3+}/8\text{-HQ}$  in the absence or presence of 50  $\mu\text{M}$  EUK-8. Arrows indicate the time points where fluorescence values were measured. (B) Summarized data showing a decrease in TMRM fluorescence over time after Fe treatment in WT ( $n = 11$ ). \*  $p < 0.05$ , \*\*  $p < 0.01$ , compared to baseline, respectively. ##  $p < 0.01$  compared between control and EUK-8 groups ( $n = 5$ ). (C) A representative MitoSOX Red fluorescence trace recorded in a WT treated myocyte with 15  $\mu\text{M}$   $\text{Fe}^{3+}/8\text{-HQ}$  in the presence of EUK-8. (D) Summarized data of MitoSOX Red fluorescence recorded from 8 WT myocytes. (E) A representative CaW trace showing the effect of pretreatment with EUK-8 on the frequency of Fe-induced CaW formation in a WT ventricular myocyte. (F) Summarized data of the frequency of CaW formation recorded from 12 myocytes.

### 3.5. IO Promoted Arrhythmias and Their Prevention by Antioxidants and mPTP Inhibition in Ex-Vivo Hearts

Cytosolic CaWs have been implicated in the generation of arrhythmias in the heart. We next evaluated the arrhythmogenic effect of IO using an ex-vivo whole-heart preparation. Representative pseudo-lead II ECGs were recorded from Langendorff-perfused hearts with normal Tyrode's solution containing 15  $\mu\text{M}$   $\text{Fe}^{3+}/8\text{-HQ}$ . The susceptibility to S1-S2 stimulation-induced arrhythmias was

evaluated. As shown in Figure 6A, while control hearts (vehicle group with 15  $\mu\text{M}$  8-HQ) showed no arrhythmias, an episode of non-sustained VT was evident in the 15  $\mu\text{M}$   $\text{Fe}^{3+}$ /8-HQ perfusion group. In another group, WT hearts were pretreated with the mPTP inhibitor CsA (1  $\mu\text{M}$ ) and then concurrently perfused with 15  $\mu\text{M}$   $\text{Fe}^{3+}$ /8-HQ. The hearts in this group were significantly protected from arrhythmogenesis by IO (Figure 6B), with only occasional PVCs being observed. Similar to findings with CsA, in CypD KO mouse hearts, there was less induction of arrhythmias (Figure 6C). Furthermore, the proarrhythmic effect of IO was also attenuated by pretreatment with the antioxidant EUK-8 that exhibits both superoxide dismutase and catalase activities (Figure 6D). As summarized in Figure 6E, WT hearts were particularly susceptible to arrhythmogenesis, represented by sustained VT, non-sustained VT, and PVCs, and had an arrhythmia score averaging  $2.00 \pm 0.37$ . Significantly lower arrhythmia scores were obtained with CsA ( $0.50 \pm 0.22$ ) and EUK-8 ( $0.67 \pm 0.21$ ) pretreatment and in the CypD KO group ( $0.33 \pm 0.21$ ).

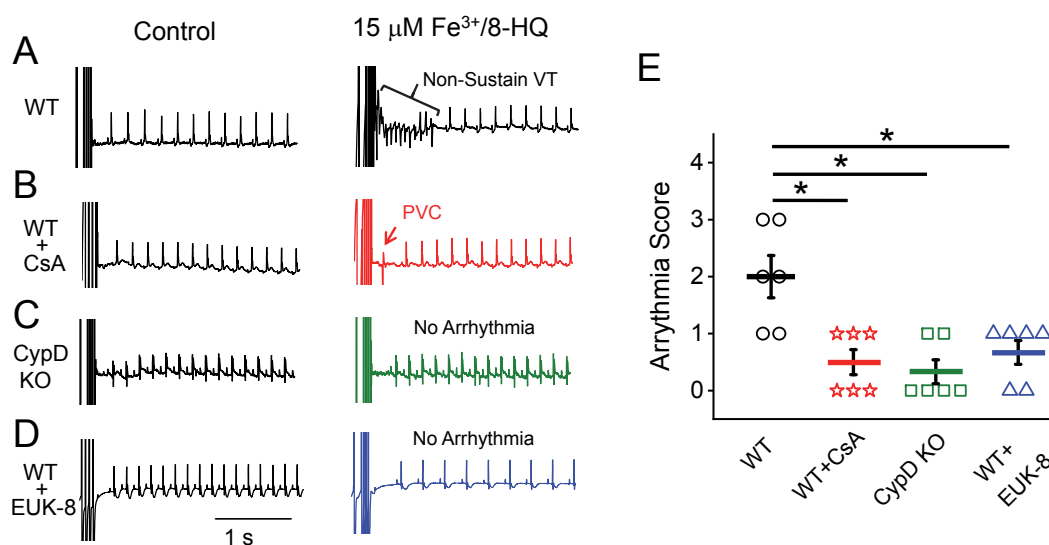


**Figure 6.** Fe-induced arrhythmias were attenuated by antioxidants and mPTP inhibition in ex-vivo mouse hearts. Pseudo-lead II ECG signals recorded from ex-vivo mouse hearts at baseline and after treatment with 15  $\mu\text{M}$  Fe/8-HQ in the presence/absence of other agents. S1-S2 programmed stimulations (as indicated by the stimulation artifacts at the beginning of each trace) were applied. (A) WT mouse heart treated with 15  $\mu\text{M}$   $\text{Fe}^{3+}$ /8-HQ. (B) WT mouse heart treated with 15  $\mu\text{M}$   $\text{Fe}^{3+}$ /8-HQ in the presence of 1  $\mu\text{M}$  CsA. (C) CypD KO mouse heart treated with 15  $\mu\text{M}$   $\text{Fe}^{3+}$ /8-HQ. (D) WT mouse heart treated with 15  $\mu\text{M}$   $\text{Fe}^{3+}$ /8-HQ in the presence of 25  $\mu\text{M}$  EUK-8. (E). Summarized arrhythmia scores ( $n = 6$  in each group). See Methods for details. \*  $p < 0.05$  compared to Fe only treatment group in WT.

#### 4. Discussion

Recent studies have revealed that IO may induce mitochondrial dysfunction [6–8]. To determine the potential link between IO and its effect on mitochondrial function and cytosolic Ca handling, we used the  $\text{Fe}^{3+}$ /8-HQ complex to iron load both cytosol and mitochondria. We have found that Fe treatment results in excess ROS generation,  $\Delta\Psi_m$  depolarization, and an increase in cytosolic CaW frequency. In agreement with the notion that cardiac arrhythmias are associated with CaWs, we have also demonstrated that IO increases the incidence of arrhythmias in ex-vivo hearts with a S1-S2 stimulation protocol. After pretreatment with CsA or in ventricular myocytes isolated from CypD KO mice, the effects of IO were alleviated, implicating an essential role of mPTP that links IO-induced  $\Delta\Psi_m$  depolarization to mitochondrial Ca efflux and CaWs/arrhythmias. Our study has not only a strong basic science component that enables us to better understand the impact of IO on mitochondrial function and Ca handling, but it also has high translational impact. We have tested possible therapeutic

approaches that might address important clinical questions related to IO-induced cardiomyopathy and cardiac arrhythmias.

#### 4.1. Iron Overload and Arrhythmogenesis—Discrepancies in Clinical and Experimental Settings

While it has been well acknowledged that IO results in cardiomyopathy [1–3], it remains unclear whether IO may play a causal role in cardiac arrhythmogenesis and how mitochondrial dysfunction might be involved [4,5]. Clinical studies have reported the occurrence of atrial and ventricular tachyarrhythmias in patients with IO conditions [4,29–34]. For example, sustained ventricular tachycardia was observed in thalassemic patients with IO [29]. Furthermore, Mancuso et al. found low voltages in ECG recordings, T wave inversions, and supraventricular arrhythmias in thalassemic patients suffering from heart failure, while their age and sex matched controls had no ECG abnormalities [30]. In addition, O in patients with sickle cell disease and hereditary hemochromatosis has been associated with the incidence of sudden cardiac death induced by severe arrhythmias [35,36]. Furthermore, Fe deposition may occur in the entire cardiac conduction system, especially the atrioventricular node, resulting in first-degree, second-degree, and complete atrioventricular block [37].

Several experimental studies have reported that chronic IO results in arrhythmias and cardiomyopathy in animal models [38,39]. For example, chronic IO has been demonstrated to result in prolonged PR intervals, heart block, and atrial fibrillation in a mouse model [38]. In addition, abnormal ECGs were present in gerbils after IO, which demonstrated prolongation of the QRS complex and PR intervals, PVCs, atrioventricular block, ST segment elevation, and T-wave inversion [39]. However, studies by Kaiser et al. have claimed that guinea pigs [40] and gerbils [40,41] do not display arrhythmias, despite showing hallmark symptoms of IO such as significant increases in cardiac and hepatic Fe deposition and cardiac and liver fibrosis. While these results imply the absence of a causal link between IO and arrhythmogenesis, their conclusions were based on spontaneously occurring arrhythmic events. The authors did not attempt to examine the effect of IO under stressed conditions such as arrhythmia induction testing, simulated hypercalcemia, or sympathetic hyperactivity ( $\beta$ -adrenergic stimulation).

In our present study, we have employed an ex-vivo cardiac model using programmed S1-S2 pacing protocols (similar to induction protocols used clinically to induce arrhythmias). While the occurrences of atrioventricular block were also noticed under IO conditions, we have focused on S1-S2 stimulation-facilitated ventricular tachyarrhythmias. We have found that IO increases the susceptibility to induced arrhythmias such as VTs in WT mouse hearts. In contrast, mPTP inhibition, either through pharmacological (CsA) or genetic intervention (CypD KO), significantly reduced the incidence of IO-induced ventricular tachyarrhythmias. These results suggest that acute IO may exert a proarrhythmic effect via  $\Delta\Psi_m$  depolarization and increased activity of mPTP, resembling our previous findings with FCCP in ventricular myocytes [19,20]. It should also be noted that IO per se may not be sufficient to readily cause arrhythmias, as other additive or synergistic factors may also be required. These factors may include elevated  $\beta$ -adrenergic stimulation, oxidative stress, and Ca overload as well as fast pacing (e.g., the programmed S1-S2 pacing as used in the present study). It remains to be further studied how other potential factors may work additively/synergistically in combination with IO conditions.

Our present proof-of-concept study has demonstrated the importance of mitochondrial function and especially mPTP in iron overload-induced Ca dysregulation and arrhythmogenesis. We acknowledge that further in-vivo experiments should provide greater insights into the overall pathological effects of iron overload as well as Fe homeostasis while allowing identification of potential compensatory mechanism(s). Further future studies using a chronic in-vivo iron overload model are warranted.

#### 4.2. Mechanisms for Ca Mishandling and Arrhythmias under IO: Roles of mPTP and Other Targets

Mitochondrial Fe is necessary for heme biosynthesis and iron-sulfur cluster biosynthesis, which are important for erythropoiesis and mitochondrial metabolism under normal physiological conditions [42]. However, excess Fe in mitochondria leads to dysfunction of these important homeostatic activities. As we discussed in our recent review article [5], it seems that IO in mitochondria plays a critical role in causing cellular oxidative stress, mitochondrial dysfunction, as well as cardiomyopathy and potentially arrhythmias. Mitochondria are located in close proximity to the SR, as well as to the calcium-releasing ryanodine receptors. This micro-domain has recently been shown to contain gradients in Ca levels [43], thus suggesting a functional relationship that involves ion fluxes between the two organelles. Our previous studies have demonstrated that FCCP-induced mitochondrial dysfunction (i.e.,  $\Delta\Psi_m$  depolarization) leads to mPTP opening that allows for mitochondrial Ca release and exacerbates CaW formation. This eventually promotes the generation of triggered activities and arrhythmias [19,20]. Since IO also induces  $\Delta\Psi_m$  depolarization, we postulate that IO could similarly promote CaWs and arrhythmias via the same mechanistic link, i.e., mPTP opening, release of Ca from mitochondria, and triggering of frequent SR Ca release (i.e., CaW formation). This postulation is supported by the evidence that inhibition of mPTP (CsA or CypD KO) attenuates IO-promoted CaWs in myocytes and arrhythmias in ex-vivo hearts.

It has been revealed that mitoferrin-1 and 2 (Mfrn1 and 2) are localized on the inner membrane of mitochondria and may play an important role in Fe uptake into the mitochondria [42,44,45]. Furthermore, a very recent report has proposed that the mitochondrial calcium uniporter (mCU) may also transport Fe into mitochondria, while Mfrn2 serves to regulate mCU transport [46]. Interestingly, some recent studies have suggested that mCUs are also involved in brain and heart mitochondrial dysfunction under IO conditions [7,29]. As summarized in our review article [47], Fe also exerts effects on ion channels in cardiomyocytes, e.g., L- and T-type Ca channels, K and Na channels. Recently, we have discovered that Fe also activates transient receptor potential canonical (TRPC) channels, which results in alterations in membrane potential, Ca handling, and cardiac dysfunction [48]. In addition, IO-enhanced ROS generation may activate calcium/calmodulin-dependent protein kinase II via oxidation and subsequently affect many ionic channels/transporters, e.g.,  $I_{Na}$ ,  $I_{CaL}$ , and RyR, and promote afterdepolarizations [11,49–51]. Therefore, it is conceivable that IO-induced cardiac dysfunction/arrhythmias may be mediated by multiple targets including ROS generation, mitochondrial function, mitochondrial and SR Ca handling, as well as sarcolemmal ion channels. A comprehensive approach may be necessary for effective prevention/treatment for IO-associated cardiac disease.

#### 4.3. IO-Induced Oxidative Stress and the Effect of Antioxidants

In agreement with the notion that Fe participates in the Fenton reactions generating free radicals, we observed a significant increase in ROS levels in mitochondria after Fe treatment. We also found that Fe caused  $\Delta\Psi_m$  depolarization in a dose-dependent manner in both WT and CypD KO. Since mPTPs are Ca, redox, voltage, and pH sensitive, their opening is promoted by free Ca in the mitochondrial matrix, ROS,  $\Delta\Psi_m$  depolarization, and an alkaline pH [52]. It has been well established that the mPTP can open in response to mitochondrial stress, including a buildup of reactive oxygen species [53,54], and ischemia-reperfusion injury [55]. It has been suggested that formation of disulfide bonds between critical thiol groups on the adenine nucleotide translocator (ANT) may facilitate CypD binding to promote mPTP opening, which may be the basis for the effects of ROS [56]. In our previous studies, we used the protonophore FCCP to dissipate the proton gradient and to directly depolarize  $\Delta\Psi_m$  in order to cause mPTP opening [19,20]. In the present study, both IO-promoted ROS generation and  $\Delta\Psi_m$  depolarization should increase the probability of mPTP opening, while CypD KO should attenuate the probability of mPTP opening. Our present results are consistent with the findings of Sripetchwandee et al., who showed that Fe is capable of generating mitochondrial ROS that then depolarize the  $\Delta\Psi_m$  and open the mPTP, resulting in mitochondrial swelling [7].

#### 4.4. Limitations

The calcein/cobalt-quenching assay has been used by other investigators and ourselves to determine the extent of mPTP opening [19,57]. However, it should be noted that mPTP opening could not be evaluated by using this assay under IO conditions as calcein fluorescence is also quenched directly by Fe. Indirect evaluation of mPTP opening by measuring mitochondrial swelling [58] may serve as another method to determine the extent of mPTP opening. In fact, a recent study from our collaborator's group has shown that exogenous Fe leads to mitochondrial swelling and mPTP opening [7]. In addition, evaluation of mitochondrial respiration using the Seahorse analyzer may also provide insights into changes in mitochondrial function under IO conditions [59]. Nevertheless, our experiments using the mPTP inhibitor CsA and CypD KO mice provide direct evidence of the role of mPTP under IO conditions.

#### 5. Conclusions

Our present study demonstrates that IO induces mitochondrial ROS generation and  $\Delta\Psi_m$  depolarization, thereby opening the mPTP and promoting CaWs and cardiac arrhythmias. Conversely, the inhibition of mPTP ameliorates the proarrhythmic effects of IO.

**Author Contributions:** Investigation, R.G., N.F.; data curation, R.G., N.F.; writing—original draft preparation, R.G., L.-H.X.; writing—review and editing, J.K.G., L.-H.X.; supervision, L.-H.X.; funding acquisition, J.K.G., L.-H.X. All authors have read and agreed to the published version of the manuscript.

**Funding:** This work was supported by the National Institutes of Health (R01s HL97979 and HL133294), the American Heart Association (19TPA34900003), and Busch Biomedical Grant to LHX.

**Conflicts of Interest:** The authors declare no conflict of interest.

#### References

- Murphy, C.J.; Oudit, G.Y. Iron-overload cardiomyopathy: Pathophysiology, diagnosis, and treatment. *J. Card. Fail.* **2010**, *16*, 888–900. [[CrossRef](#)]
- Das, S.K.; Wang, W.; Zhabyeyev, P.; Basu, R.; McLean, B.; Fan, D.; Parajuli, N.; DesAulniers, J.; Patel, V.B.; Hajjar, R.J.; et al. Iron-overload injury and cardiomyopathy in acquired and genetic models is attenuated by resveratrol therapy. *Sci. Rep.* **2015**, *5*, 18132. [[CrossRef](#)]
- Kremastinos, D.T.; Tsetsos, G.A.; Tsiapras, D.P.; Karavolias, G.K.; Ladis, V.A.; Kattamis, C.A. Heart failure in beta thalassemia: A 5-year follow-up study. *Am. J. Med.* **2001**, *111*, 349–354. [[CrossRef](#)]
- Shizukuda, Y.; Rosing, D.R. Iron overload and arrhythmias: Influence of confounding factors. *J. Arrhythmia* **2019**, *35*, 575–583. [[CrossRef](#)]
- Gordan, R.; Wongjaikam, S.; Gwathmey, J.K.; Chattipakorn, N.; Chattipakorn, S.C.; Xie, L.H. Involvement of cytosolic and mitochondrial iron in iron overload cardiomyopathy: An update. *Heart Fail. Rev.* **2018**, *23*, 801–816. [[CrossRef](#)]
- Kumfu, S.; Chattipakorn, S.; Fucharoen, S.; Chattipakorn, N. Mitochondrial calcium uniporter blocker prevents cardiac mitochondrial dysfunction induced by iron overload in thalassemic mice. *Biomaterials* **2012**, *25*, 1167–1175. [[CrossRef](#)]
- Sripetchwandee, J.; KenKnight, S.B.; Sanit, J.; Chattipakorn, S.; Chattipakorn, N. Blockade of mitochondrial calcium uniporter prevents cardiac mitochondrial dysfunction caused by iron overload. *Acta Physiol.* **2014**, *210*, 330–341. [[CrossRef](#)]
- Fedotcheva, N.I.; Mokhova, E.N. Mitochondrial models of pathologies with oxidative stress. Efficiency of alkalization to reduce mitochondrial damage. *Biochemistry* **2013**, *78*, 1293–1297. [[CrossRef](#)] [[PubMed](#)]
- Berdoukas, V.; Coates, T.D.; Cabantchik, Z.I. Iron and oxidative stress in cardiomyopathy in thalassemia. *Free Radic. Biol. Med.* **2015**, *88*, 3–9. [[CrossRef](#)] [[PubMed](#)]
- Gordan, R.; Xie, L.H. Primary effect of reactive oxygen species on electrical remodeling of the heart. *Circulation* **2014**, *78*, 1834–1836. [[CrossRef](#)] [[PubMed](#)]
- Xie, L.H.; Chen, F.; Karagueuzian, H.S.; Weiss, J.N. Oxidative-stress-induced afterdepolarizations and calmodulin kinase II signaling. *Circ. Res.* **2009**, *104*, 79–86. [[CrossRef](#)] [[PubMed](#)]

12. Munzel, T.; Camici, G.G.; Maack, C.; Bonetti, N.R.; Fuster, V.; Kovacic, J.C. Impact of Oxidative Stress on the Heart and Vasculature: Part 2 of a 3-Part Series. *J. Am. Coll. Cardiol.* **2017**, *70*, 212–229. [[CrossRef](#)]
13. Lefler, D.J.; Granger, D.N. Oxidative stress and cardiac disease. *Am. J. Med.* **2000**, *109*, 315–323. [[CrossRef](#)]
14. Bernardi, P. Modulation of the mitochondrial cyclosporin A-sensitive permeability transition pore by the proton electrochemical gradient. Evidence that the pore can be opened by membrane depolarization. *J. Biol. Chem.* **1992**, *267*, 8834–8839. [[PubMed](#)]
15. Dedkova, E.N.; Blatter, L.A. Mitochondrial Ca<sup>2+</sup> and the heart. *Cell Calcium* **2008**, *44*, 77–91. [[CrossRef](#)] [[PubMed](#)]
16. Bers, D.M. Calcium cycling and signaling in cardiac myocytes. *Annu. Rev. Physiol.* **2008**, *70*, 23–49. [[CrossRef](#)] [[PubMed](#)]
17. Halestrap, A.P.; Pasdois, P. The role of the mitochondrial permeability transition pore in heart disease. *Biochim. Biophys. Acta* **2009**, *1787*, 1402–1415. [[CrossRef](#)]
18. Ruiz-Meana, M.; Fernandez-Sanz, C.; Garcia-Dorado, D. The SR-mitochondria interaction: A new player in cardiac pathophysiology. *Cardiovasc. Res.* **2010**, *88*, 30–39. [[CrossRef](#)]
19. Zhao, Z.; Gordan, R.; Wen, H.; Fefelova, N.; Zang, W.J.; Xie, L.H. Modulation of intracellular calcium waves and triggered activities by mitochondrial Ca flux in mouse cardiomyocytes. *PLoS ONE* **2013**, *8*, e80574. [[CrossRef](#)]
20. Gordan, R.; Fefelova, N.; Gwathmey, J.K.; Xie, L.H. Involvement of mitochondrial permeability transition pore (mPTP) in cardiac arrhythmias: Evidence from cyclophilin D knockout mice. *Cell Calcium* **2016**, *60*, 363–372. [[CrossRef](#)]
21. Baines, C.P.; Kaiser, R.A.; Purcell, N.H.; Blair, N.S.; Osinska, H.; Hambleton, M.A.; Brunskill, E.W.; Sayen, M.R.; Gottlieb, R.A.; Dorn, G.W.; et al. Loss of cyclophilin D reveals a critical role for mitochondrial permeability transition in cell death. *Nature* **2005**, *434*, 658–662. [[CrossRef](#)] [[PubMed](#)]
22. Petrat, F.; Weisheit, D.; Lensen, M.; de Groot, H.; Sustmann, R.; Rauen, U. Selective determination of mitochondrial chelatable iron in viable cells with a new fluorescent sensor. *Biochem. J.* **2002**, *362*, 137–147. [[CrossRef](#)] [[PubMed](#)]
23. Rauen, U.; Petrat, F.; Sustmann, R.; de Groot, H. Iron-induced mitochondrial permeability transition in cultured hepatocytes. *J. Hepatol.* **2004**, *40*, 607–615. [[CrossRef](#)] [[PubMed](#)]
24. Kabaeva, Z.; Zhao, M.; Michele, D.E. Blebbistatin extends culture life of adult mouse cardiac myocytes and allows efficient and stable transgene expression. *Am. J. Physiol. Heart Circ. Physiol.* **2008**, *294*, H1667–H1674. [[CrossRef](#)] [[PubMed](#)]
25. Zhao, Z.; Babu, G.J.; Wen, H.; Fefelova, N.; Gordan, R.; Sui, X.; Yan, L.; Vatner, D.E.; Vatner, S.F.; Xie, L.H. Overexpression of adenylyl cyclase type 5 (AC5) confers a proarrhythmic substrate to the heart. *Am. J. Physiol. Heart Circ. Physiol.* **2015**, *308*, H240–H249. [[CrossRef](#)]
26. Wen, H.; Zhao, Z.; Fefelova, N.; Xie, L.H. Potential Arrhythmogenic Role of TRPC Channels and Store-Operated Calcium Entry Mechanism in Mouse Ventricular Myocytes. *Front. Physiol.* **2018**, *9*, 1785. [[CrossRef](#)]
27. Xie, L.H.; Weiss, J.N. Arrhythmogenic consequences of intracellular calcium waves. *Am. J. Physiol. Heart Circ. Physiol.* **2009**, *297*, H997–H1002. [[CrossRef](#)]
28. Chang, H.C.; Wu, R.; Shang, M.; Sato, T.; Chen, C.; Shapiro, J.S.; Liu, T.; Thakur, A.; Sawicki, K.T.; Prasad, S.V.; et al. Reduction in mitochondrial iron alleviates cardiac damage during injury. *EMBO Mol. Med.* **2016**, *8*, 247–267. [[CrossRef](#)]
29. Bayar, N.; Arslan, S.; Erkal, Z.; Kucukseymen, S. Sustained ventricular tachycardia in a patient with thalassemia major. *Ann. Noninvasive Electrocardiol.* **2014**, *19*, 193–197. [[CrossRef](#)]
30. Mancuso, L.; Mancuso, A.; Bevacqua, E.; Rigano, P. Electrocardiographic abnormalities in thalassemia patients with heart failure. *Cardiovasc. Hematol. Disord. Drug Targets* **2009**, *9*, 29–35. [[CrossRef](#)]
31. Cavallaro, L.; Meo, A.; Busa, G.; Coglitore, A.; Sergi, G.; Satullo, G.; Donato, A.; Calabro, M.P.; Miceli, M. Arrhythmia in thalassemia major: Evaluation of iron chelating therapy by dynamic ECG. *Minerva Cardioangiol.* **1993**, *41*, 297–301. [[PubMed](#)]
32. Heper, G.; Ozensoy, U.; Korkmaz, M.E. Persistent atrial standstill and idioventricular rhythm in a patient with thalassemia intermedia. *Turk Kardiyol. Dern. Ars. Turk Kardiyol. Dern. Yayin Organidir* **2009**, *37*, 256–259.

33. Nisli, K.; Taner, Y.; Naci, O.; Zafer, S.; Zeynep, K.; Aygun, D.; Umrah, A.; Rukiye, E.; Turkan, E. Electrocardiographic markers for the early detection of cardiac disease in patients with beta-thalassemia major. *J. Pediatr.* **2010**, *86*, 159–162. [[CrossRef](#)] [[PubMed](#)]
34. Wu, V.C.; Huang, J.W.; Wu, M.S.; Chin, C.Y.; Chiang, F.T.; Liu, Y.B.; Wu, K.D. The effect of iron stores on corrected QT dispersion in patients undergoing peritoneal dialysis. *Am. J. Kidney Dis.* **2004**, *44*, 720–728. [[CrossRef](#)]
35. Adams, R.J.; McKie, V.C.; Brambilla, D.; Carl, E.; Gallagher, D.; Nichols, F.T.; Roach, S.; Abboud, M.; Berman, B.; Driscoll, C.; et al. Stroke prevention trial in sickle cell anemia. *Control. Clin. Trials* **1998**, *19*, 110–129. [[CrossRef](#)]
36. Klintschar, M.; Stiller, D. Sudden cardiac death in hereditary hemochromatosis: An underestimated cause of death? *Int. J. Leg. Med.* **2004**, *118*, 174–177. [[CrossRef](#)]
37. Aronow, W.S.; Meister, L.; Kent, J.R. Atrioventricular block in familial hemochromatosis treated by permanent synchronous pacemaker. *Arch. Intern. Med.* **1969**, *123*, 433–435. [[CrossRef](#)]
38. Rose, R.A.; Sellan, M.; Simpson, J.A.; Izaddoustdar, F.; Cifelli, C.; Panama, B.K.; Davis, M.; Zhao, D.; Markhani, M.; Murphy, G.G.; et al. Iron overload decreases CaV1.3-dependent L-type Ca<sup>2+</sup> currents leading to bradycardia, altered electrical conduction, and atrial fibrillation. *Circ. Arrhythm. Electrophysiol.* **2011**, *4*, 733–742. [[CrossRef](#)]
39. Obejero-Paz, C.A.; Yang, T.; Dong, W.Q.; Levy, M.N.; Brittenham, G.M.; Kuryshv, Y.A.; Brown, A.M. Deferoxamine promotes survival and prevents electrocardiographic abnormalities in the gerbil model of iron-overload cardiomyopathy. *J. Lab. Clin. Med.* **2003**, *141*, 121–130. [[CrossRef](#)]
40. Kaiser, L.; Davis, J.; Patterson, J.; Boyd, R.F.; Olivier, N.B.; Bohart, G.; Schwartz, K.A. Iron does not cause arrhythmias in the guinea pig model of transfusional iron overload. *Comp. Med.* **2007**, *57*, 383–389. [[CrossRef](#)]
41. Kaiser, L.; Davis, J.M.; Patterson, J.; Johnson, A.L.; Bohart, G.; Olivier, N.B.; Schwartz, K.A. Iron sufficient to cause hepatic fibrosis and ascites does not cause cardiac arrhythmias in the gerbil. *Transl. Res.* **2009**, *154*, 202–213. [[CrossRef](#)] [[PubMed](#)]
42. Richardson, D.R.; Lane, D.J.; Becker, E.M.; Huang, M.L.; Whitnall, M.; Suryo Rahmanto, Y.; Sheftel, A.D.; Ponka, P. Mitochondrial iron trafficking and the integration of iron metabolism between the mitochondrion and cytosol. *Proc. Natl. Acad. Sci. USA* **2010**, *107*, 10775–10782. [[CrossRef](#)] [[PubMed](#)]
43. Lu, X.; Ginsburg, K.S.; Kettlewell, S.; Bossuyt, J.; Smith, G.L.; Bers, D.M. Measuring local gradients of intramitochondrial [Ca<sup>2+</sup>] in cardiac myocytes during sarcoplasmic reticulum Ca<sup>2+</sup> release. *Circ. Res.* **2013**, *112*, 424–431. [[CrossRef](#)] [[PubMed](#)]
44. Shaw, G.C.; Cope, J.J.; Li, L.; Corson, K.; Hersey, C.; Ackermann, G.E.; Gwynn, B.; Lambert, A.J.; Wingert, R.A.; Traver, D.; et al. Mitoferrin is essential for erythroid iron assimilation. *Nature* **2006**, *440*, 96–100. [[CrossRef](#)] [[PubMed](#)]
45. Paradkar, P.N.; Zumbrennen, K.B.; Paw, B.H.; Ward, D.M.; Kaplan, J. Regulation of mitochondrial iron import through differential turnover of mitoferrin 1 and mitoferrin 2. *Mol. Cell. Biol.* **2009**, *29*, 1007–1016. [[CrossRef](#)] [[PubMed](#)]
46. Nieminen, A.L.; Schwartz, J.; Hung, H.I.; Blocker, E.R.; Gooz, M.; Lemasters, J.J. Mitoferrin-2 (MFRN2) Regulates the Electrogenic Mitochondrial Calcium Uniporter and Interacts Physically with MCU. *Biophys. J.* **2014**, *106*, 581. [[CrossRef](#)]
47. Siri-Angkul, N.; Xie, L.H.; Chattipakorn, S.C.; Chattipakorn, N. Cellular Electrophysiology of Iron-Overloaded Cardiomyocytes. *Front. Physiol.* **2018**, *9*, 1615. [[CrossRef](#)]
48. Siri-Angkul, N.; Gordan, R.; Wongjaikam, S.; Fefelova, N.; Gwathmey, J.K.; Chattipakorn, S.; Chattipakorn, N.; Xie, L.H. Activation of transient receptor potential canonical channel currents in iron-overloaded cardiac myocytes. *Circ. Res.* **2019**, *125*, A507. [[CrossRef](#)]
49. Erickson, J.R.; Joiner, M.L.; Guan, X.; Kutschke, W.; Yang, J.; Oddis, C.V.; Bartlett, R.K.; Lowe, J.S.; O'Donnell, S.E.; Aykin-Burns, N.; et al. A dynamic pathway for calcium-independent activation of CaMKII by methionine oxidation. *Cell* **2008**, *133*, 462–474. [[CrossRef](#)]
50. Tomaselli, G.F.; Barth, A.S. Sudden cardio arrest: Oxidative stress irritates the heart. *Nat. Med.* **2010**, *16*, 648–649. [[CrossRef](#)]
51. Zhao, Z.; Fefelova, N.; Shanmugam, M.; Bishara, P.; Babu, G.J.; Xie, L.H. Angiotensin II induces afterdepolarizations via reactive oxygen species and calmodulin kinase II signaling. *J. Mol. Cell. Cardiol.* **2011**, *50*, 128–136. [[CrossRef](#)] [[PubMed](#)]

52. Weiss, J.N.; Korge, P.; Honda, H.M.; Ping, P. Role of the mitochondrial permeability transition in myocardial disease. *Circ. Res.* **2003**, *93*, 292–301. [[CrossRef](#)] [[PubMed](#)]
53. Wang, Y.H.; Shi, C.X.; Dong, F.; Sheng, J.W.; Xu, Y.F. Inhibition of the rapid component of the delayed rectifier potassium current in ventricular myocytes by angiotensin II via the AT1 receptor. *Br. J. Pharmacol.* **2008**, *154*, 429–439. [[CrossRef](#)] [[PubMed](#)]
54. Saotome, M.; Katoh, H.; Yaguchi, Y.; Tanaka, T.; Urushida, T.; Satoh, H.; Hayashi, H. Transient opening of mitochondrial permeability transition pore by reactive oxygen species protects myocardium from ischemia-reperfusion injury. *Am. J. Physiol. Heart Circ. Physiol.* **2009**, *296*, H1125–H1132. [[CrossRef](#)]
55. Halestrap, A.P.; Clarke, S.J.; Javadov, S.A. Mitochondrial permeability transition pore opening during myocardial reperfusion—A target for cardioprotection. *Cardiovasc. Res.* **2004**, *61*, 372–385. [[CrossRef](#)]
56. Halestrap, A.P. The Mitochondrial Permeability Transition—A Pore Way for the Heart to Die. *J. Clin. Basic Cardiol.* **2002**, *5*, 29–41.
57. Fraysse, B.; Nagi, S.M.; Boher, B.; Ragot, H.; Laine, J.; Salmon, A.; Fiszman, M.Y.; Toussaint, M.; Fromes, Y. Ca<sup>2+</sup> overload and mitochondrial permeability transition pore activation in living delta-sarcoglycan-deficient cardiomyocytes. *Am. J. Physiol. Cell Physiol.* **2010**, *299*, C706–C713. [[CrossRef](#)]
58. Halestrap, A.P.; Davidson, A.M. Inhibition of Ca<sup>2+</sup>-induced large-amplitude swelling of liver and heart mitochondria by cyclosporin is probably caused by the inhibitor binding to mitochondrial-matrix peptidyl-prolyl cis-trans isomerase and preventing it interacting with the adenine nucleotide translocase. *Biochem. J.* **1990**, *268*, 153–160.
59. Gordan, R.; Wongjaikam, S.; Fefelova, N.; Siri-Angkul, N.; Gwathmey, J.K.; Chattipakorn, N.; Chattipakorn, S.; Xie, L.H. Mitochondrial permeability transition pore, calcium uniporter, and iron overload in the heart. *Circ. Res.* **2018**, *123*, A254. [[CrossRef](#)]



© 2020 by the authors. Licensee MDPI, Basel, Switzerland. This article is an open access article distributed under the terms and conditions of the Creative Commons Attribution (CC BY) license (<http://creativecommons.org/licenses/by/4.0/>).